Study of the Long-Time Fluorescence Tail of the Green Fluorescent Protein

Pavel Leiderman,[†] Moran Ben-Ziv,[†] Liat Genosar,[†] Dan Huppert,*[,†] Kyril M. Solntsev,[‡] and Laren M. Tolbert[‡]

Raymond and Beverly Sackler Faculty of Exact Sciences, School of Chemistry, Tel Aviv University, Tel Aviv 69978, Israel and School of Chemistry and Biochemistry, Georgia Institute of Technology, Atlanta, Georgia 30332-0400

Received: December 10, 2003; In Final Form: March 7, 2004

The time-resolved optical response of the wild-type green fluorescent protein (WT-GFP) in water and D_2O was measured at room temperature by two optical techniques. The pump probe technique, with about 150 fs resolution, was used to measure the short-time response up to 150 ps. The short-time signals are similar to previously reported measurements. Time-correlated single photon counting (TCSPC) was used to measure the fluorescence of both the protonated and deprotonated emission bands of WT-GFP. The long-time fluorescence decay of the protonated form of WT-GFP decays nonexponentially. When this decay curve is multiplied by $\exp(t/\tau_f)$ where τ_f is the lifetime of deprotonated form, the long-time tail decays as a power law of about $t^{-3/2}$. Such a long-time fluorescence decay behavior represents the general emission decay pattern of excited photoacids in solutions and microemulsions and adds additional previously unrevealed information on the dynamics of this reaction. We attribute the long-time behavior to a diffusion-assisted geminate recombination process of the proton with the deprotonated species to reform the protonated chromophore.

Introduction

The green fluorescent protein (GFP) of the jellyfish *Aequorea victoria* has attracted great interest as a biological fluorescence marker and as one of the few examples of excited-state proton transfer in nature. Nevertheless, it has been widely assumed that the important information is contained in the early time (fast) behavior of such systems. We have been interested in the long time behavior in such dynamic systems, because this regime reveals important facets of the recombination behavior of the conjugate base and the diffusing proton. Thus, we elected to apply our models of excited-state proton transfer (ESPT) in homogeneous solutions[1] to this conformationally and solvent-restricted photoacid.

Excited-state proton-transfer reactions in solution provide useful models for proton transfer in general.[2−8] The development of short pulse lasers has enabled the direct measurement of ESPT reactions, and made it possible to investigate their mechanisms in more detail.[9,10] We have studied the intermolecular proton transfer from several photoacids to water and other basic solvents such as alcohols, amides, and DMSO. An important phenomenon we have uncovered is the ability to monitor, through accurate fluorescence measurements, the finite probability that the transferred proton will recombine geminately in the excited state with the deprotonated form. The transferred proton in solution is mobile and its random walk can be described by a diffusion constant D. The asymptotic long time behavior of the diffusion assisted reversible geminate recombination model leads to a power law decay of the fluorescence of the protonated chromophore

$$I_f(t)e^{t/\tau_f} \propto [K^*_{eq}/(4\pi D)^{3/2}]t^{-3/2} \quad (1)$$

where K^*_{eq} is the excited-state proton-transfer equilibrium constant and τ_f is the fluorescence lifetime of the deprotonated form. The main thrust of this study is to measure the time-resolved fluorescence of WT-GFP. As we will show in this paper, the WT-GFP long-time fluorescence tail, measured at high-energy part of the spectrum at 460 nm, has the same pattern as regular photoacids in solution, despite the restrictive geometry of the photoacid within the protein core. We explain this tail with the same formalism and model with which we treated photoacids in solution.

Formation of the wild-type chromophore (*p-hydroxybenzylidene-imidazolidinone*) occurs in the absence of cofactors via posttranslational cyclization followed by autoxidation within a tripeptide unit of the polypeptide sequence consisting of 238 amino acids.[11] X-ray diffraction revealed that the chromophore is protectively housed along a coaxial helix threaded through the center of an 11-stranded β-barrel.[12] The chromophore is covalently anchored and effectively secluded from the aqueous solvent surrounding the protein.[12,13] Additional noncovalent coupling of the chromophore to the protein backbone is facilitated via an extended hydrogen-bonded network.[14]

At room temperature, WT-GFP exhibits two main absorption peaks with maxima at 398 nm (band A) and 478 nm (band B). The ratio of the absorption bands depends on the pH. As the pH increases, the B band gets stronger. There are two emission peaks in the steady-state fluorescence spectrum, a very weak band at 460 nm and a very strong band at 510 nm.

The excited-state dynamics of WT-GFP have been studied by several groups[15−20] following photoexcitation of each of its two strong absorption bands in the visible part of the spectra using fluorescence upconversion spectroscopy (about 100 fs time

* To whom correspondence should be addressed. Dan Huppert, Raymond and Beverly Sackler Faculty of Exact Sciences, School of Chemistry, Tel Aviv University, Tel Aviv 69978, Israel. E-mail: huppert@tulip.tau.ac.il. Fax/Phone: 972-3-6407012.

[†] Raymond and Beverly Sackler Faculty of Exact Sciences, School of Chemistry, Tel Aviv University.

[‡] School of Chemistry and Biochemistry, Georgia Institute of Technology.

10.1021/jp037786i CCC: $27.50
Published on Web 05/14/2004

SCHEME 1. Cyclization and Deportation of GFP[a]

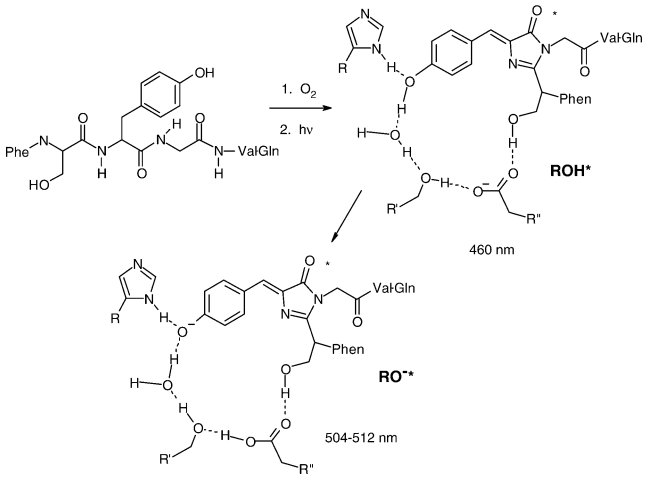

[a] Adapted from reference 14.

SCHEME 2

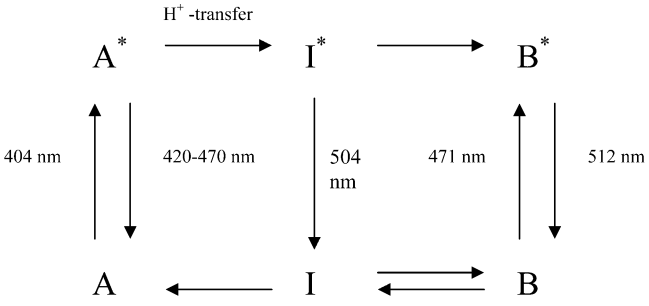

resolution) and other ultrafast techniques. Excitation of the higher energy band leads very rapidly to the lower energy species, and the excited-state interconversion rate shows a large kinetic isotope effect. Through these observations, and the dynamical studies of refs 15−21, Webb and co-workers lead to a model in which the two visible absorption bands of the WT-GFP correspond to protonated and deprotonated ground-state conformations, which we denote as $ROH_{(g)}$ and $RO^-_{(g)}$. These two weak acid states can be slowly interconverted in the ground state, but in the excited state this photoacid becomes stronger. The large isotope effect and other properties suggest that an excited-state proton-transfer reaction, followed by additional structural changes, occurs upon excitation of the ROH (see Scheme 2).

Scheme 2 shows a model proposed by Boxer and co-workers[15] for the dominant photophysical processes of WT-GFP at 77 K. After excitation of the neutral chromophore, A* (ROH* in our notation) rapidly converts to I* (RO^-*), an anionic chromophore, which is in a nonequilibrium protein environment. The 460 nm emission from the A* decay rate matches the rise in emission from I* measured at about 510 nm. The hydrogen bond network near the chromophore observed in the crystal structure of the WT-GFP is suggested to be responsible for excited-state proton transfer, ESPT.[14] When B, the ground-state deprotonated chromophore (RO^-), is excited, it emits at a slightly shifted wavelength of that of I*.

Previous time-resolved studies of GFP focused their attention on the complex decay of the emission at short times up to 150 ps,[15−20] which revealed elementary proton-transfer steps from excited chromophore to immediate surrounding bases. Another time regime is micro and millisecond dynamics, well-studied using fluorescence correlation spectroscopy,[22] which revealed dynamics of large protein molecule as a whole. In contrast, in this study we focus attention on fluorescence measurements at long times (up to 10 ns). We feel that, just as with solutions, this overlooked time frame may reflect proton random walk within the protein governed by diffusion. We find that the long time behavior of the WT-GFP fluorescence decays with a power-law of $t^{-3/2}$. This type of long time decay pattern was also observed in the fluorescence of many excited-state proton-transfer reactions to the solvent and is consistent with excited-state (adiabatic) proton return. A plausible explanation for the long-time fluorescence behavior of WT-GFP is that the transferred proton can also recombine to its original site, the hydroxyl group, of the WT-GFP excited chromophore and thus repopulate the protonated form, ROH*. Such a process results in a nonexponential decay and an asymptotic power-law decay with a slope of about −3/2.

Experimental Section

Time-resolved fluorescence was acquired using the time-correlated single-photon counting (TCSPC) technique, the method of choice when sensitivity, large dynamic range and low intensity illumination are important criteria in fluorescence decay measurements.

For excitation we used a cavity dumped Ti:sapphire femtosecond laser, Mira, Coherent, which provides short, 80 fs, pulses of variable repetition rate, operating at the SHG frequency, at the spectral range of 380−400 nm and a relatively low repetition rate of 500 kHz. A low rate might be important to excite fully relaxed WT-GFP.

The TCSPC detection system is based on a Hamamatsu 3809U, photomultiplier, Tennelec 864 TAC, Tennelec 454 discriminator and a PC-based multichannel analyzer (nucleus PCA-II). The overall instrumental response was about 40 ps (fwhm). Measurements were taken at 10 nm spectral width. The large dynamic range of the TCSPC system (more than 4 orders of magnitude) enables us to accurately determine the nonexponential photoluminescence decay profiles of the WT-GFP fluorescence.

The excitation pulse energy was reduced by neutral density filters to about 1 pJ. We checked the samples absorption prior and after time-resolved measurements. We could not find noticeable changes in the absorption spectra due to sample irradiation. The time-resolved emission decay curves of the WT-GFP samples were the same after repeatable experiments. We thus conclude that, under our irradiation condition, no sample deterioration could be detected.

For the pump−probe experiments reported, we used an amplified femtosecond Ti:sapphire laser system. In brief, laser pulses (50 fs duration, centered near 800 nm with pulse energy of ∼600 μJ) at a 1 kHz repetition rate were generated by a Ti:sapphire-based oscillator (Coherent Mira seed) and amplified by a multipass Ti:sapphire amplifier (Odin Quantronix). Samples were excited by the second harmonic of the amplified laser (∼400 nm). To obtain probe pulses we pump an OPA with the 800 nm pulses, which generates tunable IR short intense pulses of about 50 fs. The IR pulses are mixed with the 800 nm pulses in a nonlinear crystal, to obtain pulses in the range 470−570 nm.

Steady-state fluorescence spectra were taken using SLM AMINCO−Bowman-2, or a FluoroMax (Jobin Yvon) spectrofluorimeters.

We received WT-GFP samples from Prof. S. J. Remington, from the Institute of Molecular Biology, University of Oregon at Eugene. Sodium salts of 8-hydroxy-1,3,6-pyrene trisulfonate, (HPTS) and 2-naphthol-6,8-disulfonate, (2N68DS), were pur-

SCHEME 3

$$\mathrm{ROH^*} \underset{k_r}{\overset{k_{PT}}{\rightleftharpoons}} [\mathrm{RO^-}^* \ldots \mathrm{H^+}]_{(r=a)} \overset{\mathrm{DSE}}{\rightleftharpoons} \mathrm{RO^-}^* + \mathrm{H^+}$$

chased from Kodak. D_2O, 99.8% isotopically pure was purchased from Aldrich. Deionized water (resistivity > 10 MΩ/cm) was used.

WT-GFP samples of 10 mg/mL included 0.3 M NaCl were stored under refrigeration. Samples were prepared by dilution of the stock solution, with either deionized water or D_2O by a factor of about 20. The TCSPC measurements samples were placed in a 1 mm optical path length quartz cell. The absorbance at 397 nm was typically 0.1 OD.

Reversible Diffusion-Influenced Two Step Model. Previous studies of reversible ESPT processes in solution led to the development of a reversible diffusion-influenced two step model[9,10] (Scheme 3). In the continuous diffusion approach, the photoacid dissociation reaction is described by the spherically symmetric diffusion equation (DSE)[23] in three dimensions.[9,10] The boundary conditions at $r = a$ are those of the back reaction, (Scheme 3). k_{PT} and k_r are the "intrinsic" dissociation and recombination rate constants at the contact sphere radius, a. Quantitative agreement was obtained between the model and the experiment.[9,10] A detailed description of the model, as well as the fitting procedure, is given in refs 9, 10, and 24.

For the numerical fit, we used the user-friendly graphic program, SSDP (Ver. 2.63), of Krissinel and Agmon.[25] The comparison of the calculated signal with the experimental results involves several parameters. Usually, the adjustable parameters are the proton-transfer rate to the solvent, k_{PT}, and the geminate recombination rate, k_r. The contact radius, a, has acceptable literature values.[23] In this study we used $a = 5.5$ Å; the proton dissociation rate constant, k_{PT}, is determined from the exponential decay at early times of the fluorescence decay. At later times, the fluorescence decay was nonexponential due to the reversible geminate recombination. An important parameter in our model that strongly influences the nonexponential decay is the diffusion coefficient, D.

Another important parameter in the model is the Coulomb potential between the anion RO^-* and the geminate proton.

$$V(r) = -\frac{R_D}{r}; R_D = \frac{|z_1 z_2| e^2}{\epsilon k_B T} \qquad (2)$$

R_D is the Debye Radius, z_1 and z_2 the charges of the proton and anion, ϵ is the static dielectric constant of the solvent, and T the absolute temperature. e is the electronic charge and k_B is Boltzmann's constant.

We are not aware of literature-published values for the dielectric constant in the vicinity of the chromophore in WT-GFP. Gutman and co-workers[26] studied the PhoE channel by introducing a freely diffusing proton. The proton was released from an excited HPTS molecule. The best fitted reconstruction of the observed dynamics was attained when the water in the cavity was assigned $\epsilon \leq 55$, corroborating the theoretical estimation of Sansom and co-workers.[27] We used a relatively large value $\epsilon = 40$, thus $R_D = 14$ Å. Using somewhat lower values of ϵ changes the values of the adjustable parameters k_r and D, but changes only slightly the computed signal curvature and hence the quality of the experimental signal fitting.

The asymptotic expression (the long time behavior) for the fluorescence of ROH* is given by[9,28]

$$[\mathrm{ROH^*}] \exp(t/\tau_f) \cong \frac{\pi}{2} a^2 \exp(R_D/a) \frac{k_r}{k_{PT}(\pi D)^{3/2}} t^{-d/2} \qquad (3)$$

where τ_f is the excited-state lifetime of the deprotonated form RO^-, d the dimensionality of the relevant problem and all other symbols were previously defined. Equation 3 shows that the tail amplitude depends on several parameters but its time dependence is a power law of time that depends on the dimensionality of the problem. For 3 dimensions it assumes the power law of $t^{-3/2}$.

Results

Short-Time Pump−Probe Measurements. Figure 1 shows the pump−probe signal, measured at 510 nm, of a WT-GFP samples in H_2O and D_2O. The samples were excited by ~100 fs pulses at 400 nm, the second harmonic of an amplified Ti:sapphire laser. The repetition rate was at 1 kHz. The samples were placed in a rotating cell, to avoid photobleaching and thermal heating. The excitation laser beam spot diameter at the sample was about 400 μm and the excitation pulse energy was about 0.5 μJ/pulse. Table 1 gives the two exponential fitting parameters of the H_2O and D_2O WT-GFP samples.

The negative signal shows that stimulated emission gives the main contribution to the signal. Excitation of the ROH* leads to proton transfer from the chromophore to the hydrogen bond network. The signal, at the RO^- emission band of 510 nm, shows a finite rise time that mimics the formation time of the RO^-*. Our results are similar to the findings of other groups.[15,16,18] We fit the signal by a two exponential fit with a component of about 25% of the signal, which is limited by the time resolution of the laser system. The two other exponential components have about equal amplitudes in water. For water, their rate constants values are $(3.6\ \mathrm{ps})^{-1}$ and $(14\ \mathrm{ps})^{-1}$. The average time constant for the rise time of the 510 nm signal is $\langle\tau\rangle = 8.4$ ps. For D_2O we see a very large kinetic isotope effect. The immediate rise time is followed by a two exponential components. The short component has relative amplitude of 0.2 and a lifetime of 12 ps, and the long component is about 62 ps. The average time constant is $\langle\tau\rangle = 52$ ps.

Long-Time Fluorescence Measurements by TCSPC. From the reversible geminate recombination modeling and the asymptotic long time behavior, given by eq 3, it arises that the fluorescence tail of the protonated photoacid ROH* obeys a power law of $t^{-3/2}$. Figure 2 shows on a log−log plot the fluorescence decays of a commonly used photoacids, 8-hydroxypyrene 1,3,6-trisulfonate (HPTS) and 2-naphthol-6,8-disulfonate (2N68DS), in water measured at their ROH* bands. To account for the finite excited-state lifetime, the experimental fluorescence intensity is multiplied by $\exp(t/\tau_f)$ where τ_f is the fluorescence lifetime of both the RO^-* species, 5.4 ns for HPTS and 12.2 ns for 2N68DS. As seen in the Figure, the fluorescence tails decay as a straight line with a slope of about −3/2. The asymptotic long time expression, eq 3, shows that the tail intensity (but not its time dependence) depends on the Coulomb potential by the term $e^{R_D/a}$ where R_D is the Debye radius and a is the sphere radius which designates (in the spherical symmetry approximation) the molecular size of the photoacid molecule plus about one water molecule in size. Debye radius reflects the distance between the negative and the positive charges at which the thermal energy equals the coulomb energy. The deprotonated form of HPTS, RO^-, in water is negatively charged by four units of the electronic charge and $R_D \cong 28$ Å, while for the triply negatively charged RO^- of 2N68DS $R_D \cong 21$ Å.

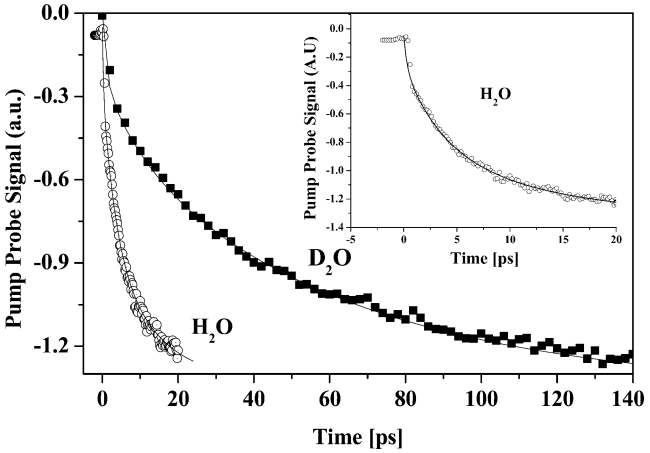

Figure 1. Pump-probe signal, measured at 510 nm, of WT-GFP in water and D_2O (dots) and the two-exponential fit (solid).

TABLE 1: Kinetic Parameters for the Proton Transfer Reaction from WT-GFP in Different Solutions Measured by Pump−Probe Technique[a]

WT-GFP	A_1	τ_1 [ps]	A_2	τ_2 [ps]	$\langle\tau\rangle$ [ps]
in D_2O	0.20	12	0.80	62	52
in H_2O	0.54	3.6	0.46	14	8.4

[a] Ex = 400 nm, probe = 510 nm.

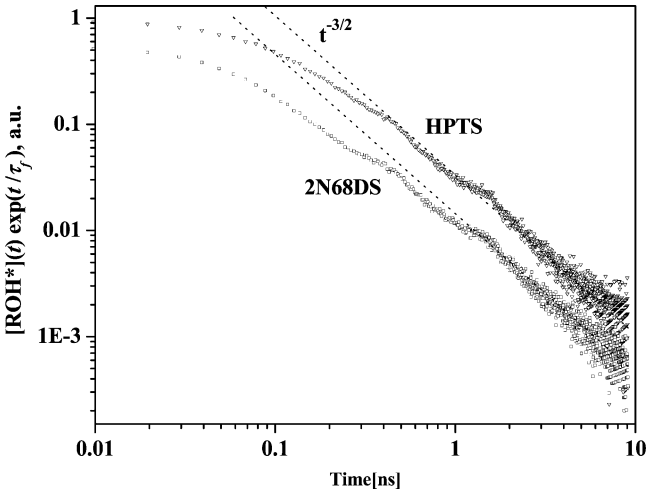

Figure 2. Log−log plot of the time-resolved emission in an aqueous solution of the ROH* photoacid form of HPTS and 2N68DS, multiplied by $\exp(t/\tau_f)$. The broken line is a fit to the asymptotic power law.

Figure 3 shows the model fit on a semilog plot of the experimental results for both HPTS and 2N68DS. The fitting parameters, given in Table 2, include the large proton diffusion constant in water $D \cong 10^{-4}$ cm^2 s^{-1} and the large dielectric constant of water $\epsilon \cong 80$. The molecular parameters are the intrinsic forward, k_{PT}, and backward, k_r, proton-transfer rate constants at the contact radius $a = 5.5$ Å and the excited-state lifetimes of both ROH* and RO$^-$*.

Figure 4 shows on a semilog plot the time-resolved fluorescence intensity measured at 450 nm of a WT-GFP sample in water and D_2O as a function of time. Note that the initial fast decay is followed by a nonexponential tail which has a measurable intensity, even at rather long times, ~10 ns. The tail intensity in a water solution at about 100 ps is about 0.1 of the peak intensity while, at 5 ns, it is about 0.001 the intensity at the peak. The initial decay of WT-GFP in D_2O solution is significantly slower than in water (see inset in Figure 4), but the long time nonexponential tail is about the same.

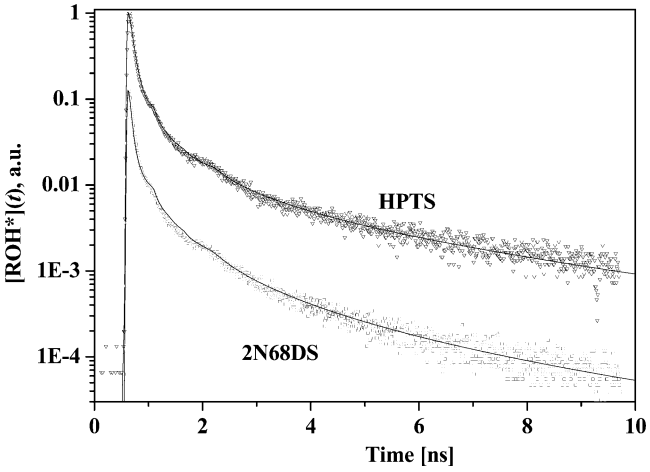

Figure 3. Diffusion-assisted model fit (solid line), using the DSE, on a semilog plot of the time-resolved emission experimental results of HPTS and 2N68DS. $D = 10^{-4}$ cm^2 s^{-1}, $\epsilon = 80$.

TABLE 2: Kinetic Parameters for the Proton Transfer Reaction of HPTS and 2N68DS in Water

	k_{PT}[a] [10^9 s^{-1}]	k_r[a,b] [10^9 Å s^{-1}]	R_D [Å]	D_{H^+} [cm^2 s^{-1}]	τ_{ROH} [ns]	τ_{RO^-} [ns]
HPTS	9.5	9	28.2	9.9×10^{-5}	5.4	5.4
2N68DS	25	20	21	9.9×10^{-5}	9.2	12.5

[a] k_{PT} and k_r are obtained from the fit of the experimental data by the reversible proton-transfer model (see text). [b] The error in the determination of k_r is 50%, see text.

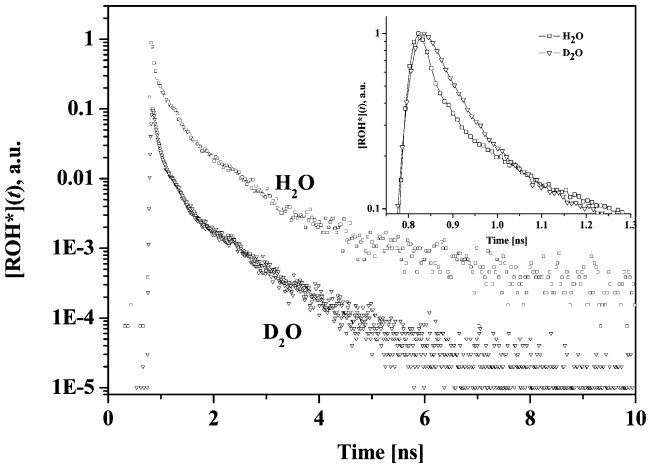

Figure 4. Time-resolved luminescence on a semilog plot of the ROH* form of WT-GFP in water and D_2O, measured at 450 nm.

Several control experiments were performed to ensure that $t^{-3/2}$ power-law asymptotic behavior in GFP is not an artifact.[29,30] Figure 5 shows on a log−log plot the time-resolved fluorescence intensity of the three WT-GFP samples displayed in Figure 4, multiplied by $\exp(t/\tau_f)$, where $\tau_f = 3.2$ ns is the excited-state lifetime of the deprotonated form of the WT-GFP emitting at wavelength $\lambda > 500$ nm. The power-law decay of $t^{-3/2}$ of the fluorescence intensity is the fingerprint of the spherical symmetrical diffusion assisted reversible geminate recombination model. The decay of the 450 nm band of WT-GFP at longer times, from about 200 ps to about 4 ns, shown in Figure 5, obeys the power law of $t^{-3/2}$. We realize that in contrast to pure solvents, where SSDP was successfully utilized to describe geminate recombination of proton and excited photobase, the GFP is a very complicated multiparameter object. Nevertheless, power-law asymptotics observed for a phenol-type GFP chro-

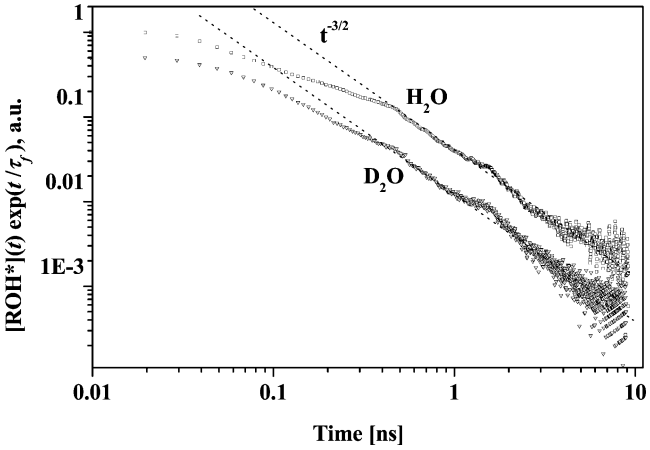

Figure 5. Log−log plot of the time-resolved fluorescence intensity of WT-GFP, multiplied by $\exp(t/\tau_f)$, $\tau_f = 3.2$ ns. The dashed curves are the asymptotic power-law of $t^{-3/2}$.

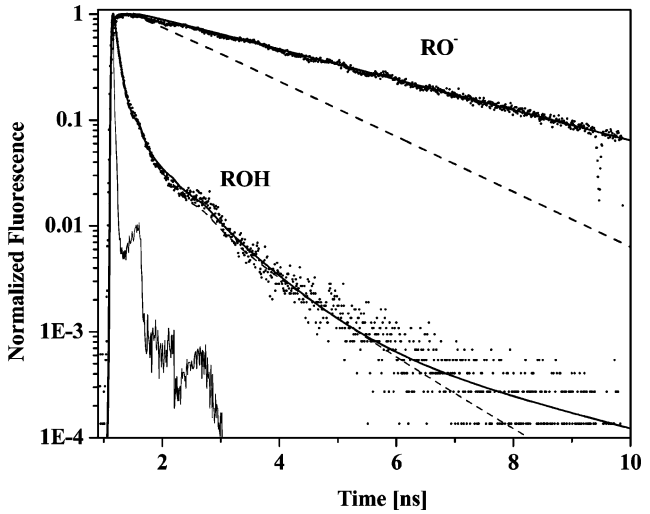

Figure 6. Time-resolved emission of the protonated chromophore of WT-GFP in D_2O, measured at 450 nm and the deprotonated form at 520 nm. Experimental results (dots), computer fit (solid line) using the diffusion assisted geminate recombination model (fitting parameters are given in Table 3).

TABLE 3: Kinetic Parameters for the Proton Transfer Reaction of WT-GFP in Different Solutions (diffusion space = 300 Å)

	k_{PT} [10^9 s^{-1}]	k_r [10^9 Å s^{-1}]	R_D [Å]	D [cm^2 s^{-1}]	τ_{ROH} [ns]	τ_{RO^-} [ns]
H_2O	70	26	14	6.5×10^{-6}	2.5	1.54
D_2O 90%	13.8	3.5	14	2.8×10^{-6}	1.67	1.67

mophore suggests a possibility of diffusion-assisted geminate recombination. So, as a possible approach toward understanding ESPT kinetics we attempted to apply the SSDP program to qualitatively describe excited-state diffusion-influenced dynamics of the GFP.

Figure 6 shows the computer fit (solid line) to the experimental time-resolved emission results (dots) of deuterated chromophore, ROD*, of the WT-GFP in D_2O, measured at 450 nm. It also shows the fit with the same parameters to the fluorescence of the deprotonated form measured at 520 nm using the reversible geminate recombination model previously described in detail. The figures show a rather good fit at all times (the fitting parameters are given in Tables 3 and 4). The initial rate of the decay depends on the deuteron transfer rate from the ROD* form to the nearby proton acceptor. From the fitting parameters, see Table 2, the deuteron transfer rate for D_2O is $(70 \text{ ps})^{-1}$. This rate has similar values (see Tables 1 and 2) to the longer component of the better time-resolved pump−probe experiments. The pump−probe signal nonexponential kinetics we found in this study of WT-GFP in D_2O corresponds to the results of Michel-Bayerle and co-workers[16] and Boxer and co-workers.[15]

We achieved a good fit to the experimental data shown in Figure 6 with two problematic fitting parameters. The first concerns the size of the diffusion space. In fitting the fluorescence of ESPT from regular photoacids such as HPTS, in bulk solution sufficiently large diffusion space (several hundred Å) mimics "infinite" separation of reactants. The outer sphere radius we use in the fit of Figure 6 is large, 300 Å; it is much larger than the size of the protein. For the WT-GFP ESPT simulations we therefore need to take a limited diffusion space that will fit the actual size of the barrel like WT-GFP. The second problem we have found in the fitting parameters is the necessity for use of an effective shorter lifetime of the RO^-*, $\tau_{eff} = 2$ ns (dashed line in Figure 6). This value is shorter than the measured lifetime $\tau_{RO^-} = 3.2$ ns. In the discussion section we explain in detail the fitting procedure and also use successfully more realistic parameters to fit the ROH* fluorescence decay curves of WT-GFP in water and D_2O.

We also plot, in Figure 6, the instrument response function, which has a 40 ps fwhm. It also includes two broad low intensity "bumps" in the response function at about 200 ps and at about 1 ns, with relative peak intensities of 0.01 and 0.001. These bumps are also superimposed on the experimental fluorescence signal. Convolution of the instrument response function with the computed DSE ROH* population also generates these two peaks of the instrument response function in the computed signal. Using the reversible geminate recombination model to calculate both ROH*(t) and RO^-*(t), shows rather a good fit.

Discussion

Short-Time Measurements. In the study of wild-type GFP fluorescence Boxer and co-workers[15] focused their attention on the short time range up to 150 ps. Michel-Beyerle and co-workers[16] measured the time-dependent GFP fluorescence using a streak camera and by time-correlated signal photon counting techniques. The streak camera results of the protonated form of the GFP are provided up to several hundred picoseconds. Vohringer and co-workers[18] used pump−probe technique and measured the GFP signal over a large spectral range with a high time resolution but at a relatively short time range. Figure 1 shows the pump−probe signal measured at the WT-GFP RO^- emission band maximum, 510 nm. We fit the signal with two exponentials and an immediate component. We measured the signal for both the H_2O and D_2O WT-GFP samples. Our results are similar to the results of other ultrafast measurements.[15,16,18] From the results, two important conclusions can be drawn. In water, the two components, $\tau_1 = 3.6$ ps and $\tau_2 = 14$ ps, have about the same amplitude while, in D_2O, the amplitude of the short component, $\tau_1 = 12$ ps, is only about a quarter of the long one, $\tau_1 = 62$ ps. The second result is the relatively large isotope effect. For the ESPT process of photoacids in bulk aqueous solution, we find an isotope effect of about 3 and for super-photoacid it is less than 3.[31] In the WT-GFP, we found[7] for the average time constants an isotope effect of $52/8.4 \cong 6.3$ and for the long component $62/14 \cong 4.4$. Such large isotope effect could be an evidence for multistep proton transfer.[32]

Long-Time Measurements. Our major objective in this study was the accurate measurement and analysis of the long-time

TABLE 4: Kinetic Parameters for the Proton Transfer Reaction WT-GFP in Different Solution with Partially Reflective Boundary Condition Diffusion Space = 17 Å

(a) Larger Diffusion Constant

	k_{PT} [10^9 s^{-1}]	k_r [10^9 Å × s^{-1}]	R_D [Å]	D [cm^2 s^{-1}]	$\tau_{eff\ ROH}$ [ns]	τ_{RO}[a] [ns]	k'_r[b] [10^9 s^{-1}]	k'_d[c] [10^9 Å × s^{-1}]	$\tau_{surface}$[d] [ns]
H_2O	70	42	14	2.5×10^{-5}	2.5	3.12	34	0.25	1.67
D_2O 90%	15	4.5	14	9.0×10^{-6}	2.5	3.12	12	0.1	1.67

(b) Smaller Diffusion Constant

	k_{PT} [10^9 s^{-1}]	k_r [10^9 Å × s^{-1}]	R_D [Å]	D [cm^2 s^{-1}]	τ_{ROH}[a] [ns^{-1}]	$\tau_{eff\ RO^-}$ [ns]	k'_d[b] [10^9 s^{-1}]	k'_r[c] [10^9 Å × s^{-1}]	$\tau_{surface}$[d] [ns]
H_2O	70	35	14	9×10^{-6}	2.5	1.82	34	0.5	1.67
D_2O 90%	15	2.5	14	3×10^{-6}	2.5	2	12	0.2	1.67

[a] We estimate the τ_{ROH} from low-temperature measurement. [b] Proton recombination rate constant at the outer surface. [c] Proton dissociation rate constant at the outer surface. [d] Effective lifetime of a proton at the surface.

fluorescence of the protonated form of WT-GFP. As seen in Figures 4-5, we found that the fluorescence tail, (200 ps − 10 ns), of ROH*, the protonated form of the WT-GFP in water and ROD* in D_2O, measured with TCSPC techniques, continued to be highly nonexponential. We excited the samples with 80 fs pulses over the spectral range of 380−400 nm of a Ti:sapphire cavity dumped system with a repetition rate of 500 kHz. This rate was about 150 times slower than the free running rate of CW mode-locked Ti:sapphire lasers. The slow rate of sample excitation may provide the reason for capturing the long-time nonexponential fluorescence tail. If the ground-state reprotonation process, $RO^-_{(g)} + H^+ \rightarrow ROH_{(g)}$, where $RO^-_{(g)}$ and $ROH_{(g)}$ are the two forms of the ground-state chromophore, were slower than about 10 ns and also if the protein conformational changes that are involved in both the chromophore excitation and the proton-transfer processes both in the ground and excited state were slow, then excitation at 76−82 MHz (the usual free running rate) would be too fast for the WT-GFP to fully relax between adjacent excitations. As seen in Figure 5, if the tail intensity were multiplied by $\exp(t/\tau_f)$, where τ_f is the RO^-* lifetime of about 3.2 ns, the decay was a power law of $t^{-3/2}$. In several previous studies, on the proton transfer from photoacids to solvents, we have found that the nonexponential fluorescence tail is the fingerprint of proton transfer from photoacids to the solvent (see also Figures 2 and 3). The geminate recombination model, which was previously described in a separate section, included the finite probability of the reversible geminate recombination process of the proton from the solvent with the deprotonated form, RO^-*: $RO^-* + H^+ \rightarrow ROH*$, to reform the parent compound, ROH*, in its excited state. Such a process increased the population of ROH* and hence enhanced the fluorescence tail intensity at a given time. The overall effect was a nonexponential decay of the ROH* form. To experimentally observe the power law dependence, two favorable conditions should be met. The first requirement is relatively fast protolytic dissociation. Fluorescence kinetics of "slow" photoacids such as 2-naphthol, for which $k_{PT} \approx 0.1$ ns^{-1}, decay exponentially for more than 3 orders of magnitude, and the successive transformation into the power law remains undetected. The second requirement is a relatively long lifetime of RO^-*, as compared to the overall ROH* decay.[33] If the RO^-* has a larger fluorescence rate constant than k_d, other asymptotic behaviors, which have also been experimentally observed, are predicted.[34] The WT-GFP chromophore satisfies both conditions, and thus we expect to observe an asymptotic $t^{-3/2}$ power law decay for the ROH* fluorescence.

The structure of WT-GFP is an 11-stranded β-barrel, forming a nearly perfect cylinder 42 Å long and 24 Å in diameter.[14] The chromophore intervenes in the middle of this central helix, where it is highly protected from the bulk solvent by the surrounding β-strands. The positioning of the chromophore and its inaccessibility probably account for the small Stokes shift, for the high fluorescence quantum yield, and for the inability of O_2 to quench the excited state.[14]

SCHEME 4

$$ROH + B_1 \rightleftharpoons RO^- + {}^+HB_1$$
$${}^+HB_1 + B_2 \rightleftharpoons B_1 + {}^+HB_2$$
$$\vdots$$
$${}^+HB_{N-1} + B_N \rightleftharpoons B_{N-1} + {}^+HB_N$$

A simple model for the geminate recombination of a proton with the chromophoric unit in the WT-GFP protein can be thought of as a relay reaction between the phenol group chromophore and the relevant proton accepting groups surrounding the chromophore. If these reactions can be described as a one-dimensional stepwise reaction chain without branching, then one can model it with proper forward and backward rate constants, as seen in Scheme 4, where $B_1...B_N$ are the proton accepting functional groups of the protein and the few water molecules that also serve as proton accepting and donating groups in the barrel-like structure of the WT-GFP.

If the rate constants of the relay reactions are approximately equal, then, for a first approximation we can assign an effective single rate constant.[35,36] If the chain is long enough and the proton acceptors along the chain have equal strength, such that the proton is not anchored to a single specific site, then we can assign an effective proton diffusion constant rather than a rate constant and we can use the Debye−Smoluchowski equation in one dimension to mimic the proton-transfer process from the chromophore to the proton accepting groups and vice versa. The DSE can be solved with similar initial and boundary conditions to those used for excited-state proton transfer in bulk water. Figure 7 shows the DSE numerical solution of the fluorescence of ROH* of WT-GFP for such a relay reaction in one dimension. The slope of the log−log plot derived from the model shows that the ROH* form decays nonexponentially and the asymptotic long-time behavior decays as a power law of $t^{-1/2}$. If the actual proton-transfer relay reaction is more complex than that shown in Scheme 2, then the decay will have a power-low larger than $t^{-1/2}$. For a more branched proton-transfer scheme, where, for example, the bases $B_1...B_N$ can transfer a proton to other bases, e.g., B_1 transferring a proton to B'_1 and

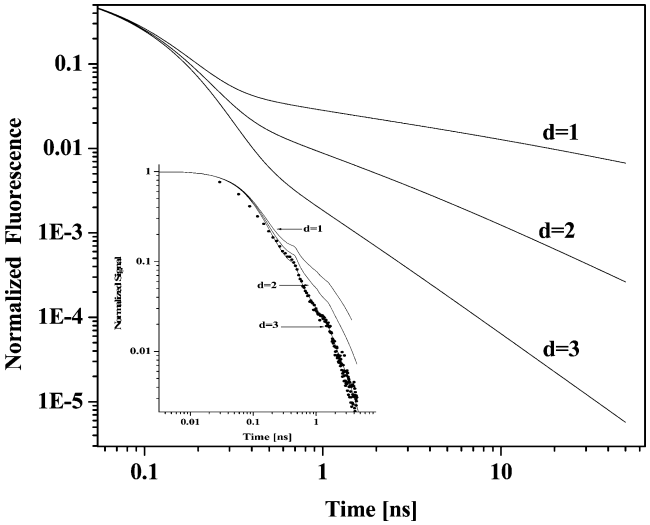

Figure 7. Simulations on a log−log plot of the time-resolved fluorescence of ROH*, multiplied using $\exp(t/\tau_f)$, by the diffusion-assisted geminate recombination model in 1, 2, and 3 dimensions. Inset—fit of the experimental data with $d = 3$.

B_2 to B'_2 etc., the proton acceptors can form a two-dimensional grid. This two-dimensional proton accepting system can be described by a two-dimensional Debye−Smoluchowski equation. The log−log plot of the DSE solution in two dimensions shows a larger nonexponential decay and the power law is t^{-1}. Figure 7 shows a log−log plot of 1, 2, and 3 dimensions simulations of the fluorescence of the ROH* form of WT-GFP using the numerical solution of Debye−Smoluchowski equation. We find a rather good fit to the experimental results of WT-GFP when we use the three-dimensional spherical symmetrical DSE with proper initial and boundary conditions, appropriate for describing a diffusion-assisted reversible proton geminate recombination process in a manner similar to our previous studies of common photoacids in solution (see Figures 5 and 6). The customary approach in chemical kinetics is to solve ordinary differential equations, namely, the rate equations. Biexponential decay is predicted from the following kinetic scheme. For proton transfer and other reactions one often writes the following kinetic scheme

$$AB \underset{k_2}{\overset{k_1}{\rightleftharpoons}} A^- + B^+$$

The molecule AB first dissociates into A and B. k_1 and k_2 are the dissociation and recombination rate constants. Historically, predictions from the kinetic approach were compared with steady-state results of DSE. This kinetic scheme leads to a biexponential decay. More complex schemes of ion-pair separation suggested by Eigen and co-workers[37] also lead to biexponential decay. In a previous paper[10] we compared Eigen's Model with our proton transfer model based on the DSE. We found that ROH* HPTS fluorescence decay does not fit well to a biexponential decay. We checked the possibility that the fluorescence decay of the ROH* form of the chromophore fit to a biexponential decay. We find large deviation between the experimental result and the computed biexponential fit at the time range up to about 2 ns. At longer times, the fluorescence signal decays almost exponentially since the excited-state radiative exponential decay dominates the signal decay.

We believe our model is not a unique description of the actual proton transfer processes that take place in the WT-GFP excited state, but certainly provides a reasonable fit to the experimental data.

Another plausible mechanism that probably affects the WT-GFP luminescence is protein conformation dynamics. Fraunfelder et al.[38] studied myoglobin (Mb) using Visible and FTIR techniques. A protein molecule possesses many conformational substates, nearly isoenergetic structures performing the same function but possibly with different rates. Agmon and Hopfield[39] simulated the dynamics of CO rebinding in myoglobin incorporating the protein conformational dynamics in the problem. The conformational dynamics were treated by a diffusion constant.

Both the forward and backward proton-transfer reactions of WT-GFP (Scheme 3) may depend on the protein conformational dynamics. The recombination reaction in such a case depends on a time-dependent conformational coordinate. In such a case, protein conformational dynamics affect the proton-transfer reactions in WT-GFP. It can also control the initial proton-transfer step $ROH^* \rightarrow RO^{-*} + H^+$. This reaction might depend on protein conformation dynamics as well, thus instead of a single rate for both the first step of proton transfer and the geminate recombination rate we expect to measure a distribution of rates when exciting a large ensemble of WT-GFP proteins. Indeed, all the time-resolved spectroscopic measurements in the ultra-short time range of excited WT-GFP, report highly nonexponential dynamics for the initial proton-transfer rate. Vohringer[18] explains and fit the pump probe signals in terms of two coordinates and three excited states: ROH*, RO^{-*} and an excited state that is not involved in proton transfer using a simple rate equation formalism. Vohringer fits the multiexponential signals of the first 20 ps for WT-GFP in water at all wavelengths with his model.

Diffusion. In this subsection, we wish to comment on the connection between one of the experimental fitting parameters, the proton diffusion constant, D, and the structure and finite size of the WT-GFP. As has been observed[14] the chromophore positioned at the barrel center is isolated from the solvent by the unique β-sheet barrel structure. Thus, according to our geminate recombination model, the transferred proton hops first from the initial site, the phenol, to a nearby water molecule, w-22,[14] and then it hops through the hydrogen bond network within the protein (see for example Figure 2 of ref 14).

Several parameters control the shape of the ROH* fluorescence as a function of time. Equation 3 gives, for the case where the proton diffuses in an infinite large volume, the asymptotic long-time behavior. The tail intensity depends on several important parameters, τ_f, a, R_D, k_d, k_r, and D. Over a very long-time, the time-dependent shape depends only on $t^{-3/2}$ (for 3 dimensions) but the intensity of the fluorescence tail depends on all the parameters mentioned above. Thus, one can fit the long-time data with a large range of these parameters. In the general case of a photoacid in solution the known parameter includes dielectric constant, molecular size and the mutual diffusion constant, $D = D_{H+} + D_{RO^-}$, and thus the "only" free adjustable parameter that determines the medium and long time behavior is the recombination rate constant, k_r.

Unlike the case of a photoacid in water, in fitting the WT-GFP fluorescence nonexponential tail, once we determine the "effective" dielectric constant, we are left with only two adjustable parameters, k_r and D. We cannot independently determine the values of both k_r and D. Thus, we are left with a range of possible values of both D and k_r. From the fitting of the experimental fluorescence we find a range of diffusion constants, $D = 2 \times 10^{-6} - 2 \times 10^{-5}$ cm^2 s^{-1} and the corresponding values of k_r are in the range 3−13 Å ns^{-1}. For a low value of $D = 2 \times 10^{-6}$ cm^2 s^{-1}, the corresponding values

of k_r is also small $-$ 3 Å ns^{-1}, and for a large value of $D = 1 \times 10^{-5}$ cm^2 s^{-1}, $k_r = 13$ Å ns^{-1}, see Tables 3 and 4.

Due to the finite size of the protein, we used the DSE with limited diffusion space. We placed an external spherical surface at a proper distance from the origin. We find that in a limited small diffusion space there is a large difference between the calculated fluorescence signal using a large or small value of *D*. The volume of the WT-GFP, with its cylindrical symmetry of 24 × 42 Å, matches the volume of a sphere with a radius of about 17 Å. Since we used a spherical symmetric model, for the DSE fluorescence calculation, we placed an outer sphere boundary at a radius of $R = 17$ Å.

When *D* is large, $D \geq 1 \times 10^{-5}$ cm^{2}s^{-1}, the proton moves fast and reaches the outer sphere (the protein's boundaries) in a relatively short time. In this case, the outer surface boundary conditions are important and strongly influence the long-time fluorescence tail.[40] The outer surface boundary conditions include three adjustable parameters, k'_r, k'_d and τ_{sur}, k'_r and k'_d are the proton recombination and dissociation rates with the surface, respectively. τ_{sur} is the proton's effective lifetime at the surface (when the proton escapes the barrel to the bulk water, then $\tau_{sur} < \tau_{RO^-}$). We find that we can fit the fluorescence tail with boundary conditions at the outer sphere that include a rather large recombination rate of the proton to the surface, k_r, whereas the dissociation rate of the proton from the surface, k_d, back to the diffusion space is small. The proton lifetime on the surface, $\tau_{sur} \cong 2$ ns, is slightly shorter than the RO$^-$* lifetime. Thus, the captured proton sticks, for rather a long-time, to the outer boundaries of the protein. Figure 8a shows the computer fit to the WT-GFP ROD time-resolved emission band, measured at 450 nm, using the DSE with an exterior spherical surface placed at 17 Å and a large diffusion constant $D = 9 \times 10^{-6}$ cm^2 s^{-1}. In the fit, shown in Figure 8a, we used $\tau_{RO^-} = 3.2$ ns, $k'_r = 12$ Å ns^{-1} and $k'_d = 0.1$ ns^{-1} for the partially absorbing boundary conditions at 17 Å. To the figure, we also added the fluorescence calculations for two limiting boundary conditions at the outer spherical surface, the totally reflecting and absorbing boundary conditions. As is clearly seen in Figure 8a, these two extreme boundary conditions significantly change the long-time emission tail and thus for large *D*, the outer surface position and boundary condition needs to be taken into account in the fitting procedure.

When *D* is small, $D = 2 \times 10^{-6}$ cm^2 s^{-1}, the proton moves relatively slowly and thus the probability to find a proton at the outer boundary surface is small, even over the longest times, where we still monitor a significant fluorescence signal (up to about 5 ns). In this case, changing the outer surface boundary conditions from reflecting to absorbing does not appreciably affect the fluorescence tail. We cannot find values for both k_r and D to fit the experimental curve when we use the true value for the RO$^-$* lifetime as measured at 510 nm, $\tau_{RO^-} = 3.2$ ns, but we get a very good fit to the time-resolved emission experimental data only with a smaller effective decay time of RO$^-$*, $\tau_{eff} = 2.0$ ns. Figure 8b shows the fit of the same experimental results shown in Figure 8a, but with a small value of $D = 2 \times 10^{-6}$ cm^2 s^{-1} and all other parameters are the same, except τ_{RO^-} . To get a good fit, we used an effective lifetime for RO$^-$*, $\tau_{eff} = 2.0$ ns (solid line). If we use the measured value $\tau_{RO^-} = 3.2$ ns, then we cannot fit the fluorescence at long-times (dashed curve). To the figure we also added the calculated curves for two limiting boundary conditions at the outer spherical surface, the totally reflecting and absorbing boundary conditions. As seen in the figure, these two extreme boundary conditions have almost no effect on the long-time calculated fluorescence tail. This is expected since the protons (deuterons) move slowly, and hence only a small fraction of protons reaches the outer surface about 5 ns after excitation. In the next subsection we present a plausible explanation for the shorter effective lifetime of RO$^-$*.

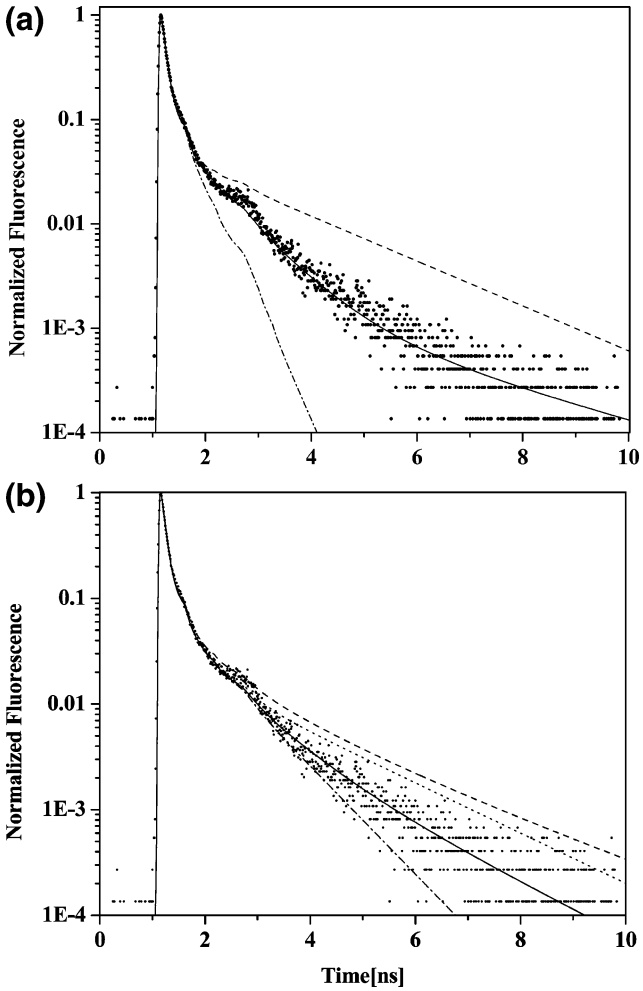

Figure 8. Computer fit to the ROH* emission of WT-GFP measured at 450 nm using the DSE in a confined diffusion space, $R = 17$ Å, in 3 dimensions. (a) $D = 8.0 \times 10^{-6}$ cm^2 s^{-1}, $\tau_{eff} = 2.0$ ns, reflecting boundary (dash line), absorbing boundary (dash dot line) and partially absorbing boundary conditions (solid line). (b) $D = 2.5 \times 10^{-6}$ cm^2 s^{-1}, absorbing boundary (dash dot line), partially absorbing boundary conditions (solid line), reflective boundary (dot) and reflecting boundary with a diffusion space of 300 Å and $\tau_{RO^-} = 3.2$ ns (dash line).

Introduction of a Base to the Photoacid and WT-GFP Solutions. When a base is introduced to a solution of strong photoacids, it can react with either the ejected proton in solution or abstract the proton by direct reaction with the excited photoacid itself. Remington[14] pointed out that the chromophore and the interior of the WT-GFP are relatively protected from the solvent. Thus, water and other large ions or molecules cannot permeate to the region of the chromophore within the excited-state lifetime, $\tau_{RO^-} = 3.2$ ns. Introducing a base in a solution of WT-GFP can show several aspects of these important properties emerging from the protein barrel structure. Introducing a base in a WT-GFP solution may or may not affect the proton-transfer reaction to the hydrogen network and the proton geminate recombination process in excited WT-GFP. We also use the example of a photoacid in solution that contains a base to demonstrate the shorter effective lifetime of the RO$^-$ form of WT-GFP needed in the fitting procedure.

Mild bases do not react with a ground-state ROH of a weak photoacid which is a weak acid (p$K \approx 7$). In the excited state,

the acidity of a photoacid increases by about 7 pK units, pK* ≈ 0. In studying the effect of a mild base on the fluorescence of a strong photoacid we observe two limiting cases: at low enough base concentrations (<30 mM), excited strong photoacids (pK* < 1, $k_{PT} > 5 \times 10^9$ s^{-1}) are capable of transferring a proton to the solution prior to the direct attack of the base, ROH + B → RO$^-$ + BH$^+$. In this case, the photoejected proton in solution can subsequently react with the base (see Scheme 5).

The initial slope of the fluorescence decay of the ROH* is not affected by the low concentration of the base in solution while the tail intensity is dramatically reduced. The reaction in solution of the base, B, with the ejected proton is fast, reaching at low base concentrations the diffusion controlled rate constant limit, k_D

$$k_D \simeq 4\pi N' D R_D \tag{4}$$

where $N' = N_A/1000$, and N_A is the Avogadro number. Since proton diffusion in an aqueous solution is large, $D \cong 10^{-4}$ cm^2 s^{-1}, the second order rate constant for negatively charged bases such as acetate or $H_2PO_4^-$, $R_D = 7.1$ Å, is of the order of 5×10^{10} M^{-1} s^{-1}. We studied the time-resolved fluorescence of the ROH* form of photoacids in the presence of a base at low concentrations.[41] We successfully used the DSE under appropriate initial and boundary conditions. We obtained a semiquantitative fit to the experimental luminescence curves of HPTS at various low concentrations of the acetate anion. The overall effect of a base on the luminescence is a strong reduction of the long-tail intensity of the ROH form without significantly affecting the initial decay which signifies the proton-transfer rate from ROH* to the solvent. The parameter that was used to introduce the proton scavenging process was the effective lifetime of the RO$^-$

$$\tau^{-1}_{\text{eff}} = \tau^{-1}_{\text{RO}^-} + k_{SC} \tag{5a}$$

$$k_{SC} = k'_{SC}[C_{SC}] \tag{5b}$$

where C_{SC} is the scavenger concentration. At low concentrations (<30 mM) of acetate in aqueous solution we obtained a good fit when we used the bimolecular rate constant $k'_{SC} = 5 \times 10^{10}$ M^{-1} s^{-1} and scavenger concentration, C_{SC}. Figure 9, parts a and b, shows the time-resolved fluorescence of HPTS and 2N68DS respectively in pure water and solutions containing KH_2PO_4 (KDP) at various concentrations. As seen in the figures, the intensity of the long-time fluorescence tail strongly decreases in the presence of relatively small concentrations of $H_2PO_4^-$.

When the base concentration is larger than 30 mM, the direct reaction of a base with the excited acid is already effective even within the short time window limited by the rate of direct proton transfer to the solvent. At higher concentrations of a base, >0.25 M, the short time initial decay rate of the fluorescence of HPTS or 2N68DS ROH* increases as a consequence of direct proton abstraction from ROH* by the base. We studied the bimolecular irreversible diffusion-assisted proton-transfer reaction ROH* + B → RO$^-$* + BH$^+$ using the celebrated "Smoluchowski theory".[42]

Figure 9c shows the time-resolved emission, measured at 450 nm, of the ROH band of the WT-GFP chromophore in an aqueous solution containing various amounts of KH_2PO_4. The effect of a base on the fluorescence curve is to increase the tail intensity. It is in the opposite direction to the effect observed on the fluorescence of a photoacid in bulk solution containing a base (see Figure 9a and b). We measured the fluorescence

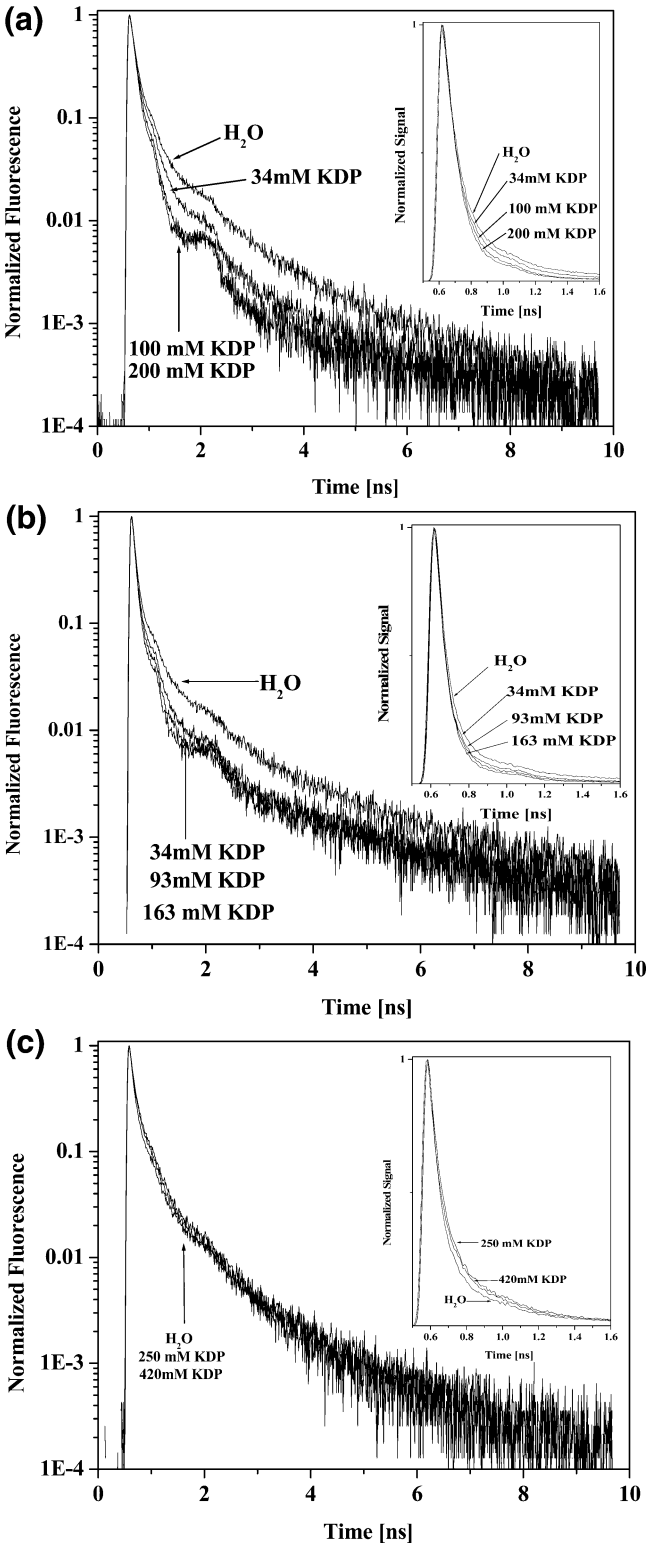

Figure 9. Time-resolved emission of the ROH band in the presence of KH_2PO_4 (KDP) in solution. Concentrations of KH_2PO_4 are marked on the figure: (a) HPTS (b) 2N68DS (c) WT-GFP.

decay of WT-GFP at several concentrations of $H_2PO_4^-$ up to a high concentration of about 400 mM. At this high concentration, we expect to capture effectively a proton that reaches the bulk solution. Unlike the experiments of photoacids in bulk solution, the WT-GFP fluorescence is only slightly affected by the base, even at high concentrations of about 0.4 M. If the barrel is permeable to large size ions such as $H_2PO_4^-$, then we would also expect a reaction with the proton that was transferred to

the hydrogen network within the barrel. We therefore conclude that within the time window of our observation, ~5 ns, we have no indication that the transferred proton reached the bulk solution or that the $H_2PO_4^-$ ion got into the barrel and captured the proton within the protein. We also used several other bases such as acetates anions, imidazole and F^-. In all of these experiments we did not find any significant effect on the time-resolved emission curve of WT-GFP ROH form, measured at 450 nm.

Another aspect of the effect of a base on a photoacid concerns the effective lifetime of the decay of the long-time fluorescence tail of WT-GFP. As previously mentioned, we failed to get a good fitting of the experimental time-resolved fluorescence curve when we used a small diffusion constant and $\tau_{RO^-} = 3.2$ ns. To get a good fit, we used an effective lifetime for RO^-*, τ_{eff}. As described above, we previously[41] used the DSE to calculate the effects of proton scavenging as well as those of direct proton transfer from a photoacid to a base on the time-resolved ROH* luminescence. Thus, applying the abovementioned proton scavenging procedure to the fitting of the emission of the ROH* form of WT-GFP, shows that there is a finite probability that a proton transferred from the chromophore to the hydrogen bonding network will find a strong enough base and, as a consequence of the proton reaction, will be locked to the base for a relatively long-time, longer than the RO^-* lifetime of about ~3 ns. In this case the "effective" lifetime of RO^-*, τ_{eff}, will be shorter than the measured decay time of the RO^-* emission band at >510 nm. We found that the best fit of the long-time emission tail is for $\tau_{eff} = 2$ ns instead of $\tau_{RO^-} = 3.2$ ns. This indicates that a relatively strong accepting group might exist a relatively short distance from the chromophore, such that the proton reacts with it at times shorter than $\tau_{RO^-} = 3.2$ ns.

Summary and Conclusions

While previously reported time-resolved studies of GFP direct their attention to the complex decay of the emission over short times up to 150 ps,[15−20] in this study we focus on fluorescence measurements over longer times (up to 10 ns). Using the TCSPC technique with a dynamic range of about 4 decades and extending the monitoring range of the emission to much longer times, we found that the fluorescence decay of ROH is nonexponential up to 10 ns. Moreover, the long-time WT-GFP fluorescence decays with a power-law of $t^{-3/2}$. This type of long-time decay pattern was also observed in the fluorescence of many excited-state proton-transfer reactions to the solvent.

We used our reversible geminate recombination model (Scheme 3) to fit the fluorescence data of WT-GFP samples. A plausible explanation for the proton transfer from excited WT-GFP is that the proton is transferred to proton accepting groups, mainly carboxylate groups, and also the few water molecules that are close to the chromophore. Since the proton hops from one proton acceptor site to others, under certain circumstances its motion can be approximately described by a random walk in three dimensions and hence a diffusion constant can be assigned to such a motion. The proton can also recombine to its original site, the hydroxyl group, of the WT-GFP chromophore and thus repopulate the protonated form, ROH*. Such a process causes a nonexponential decay and asymptotic power-law decay with a slope of about −3/2.

Acetate and $H_2PO_4^-$ are mild bases that do not react with weak acids such as the ground state protonated form, ROH, of HPTS or 2N68DS, but react effectively with the transferred proton and with the excited photoacid. This situation refers to the discussion following Scheme 5. By introducing a mild base into the WT-GFP solution and monitoring its effect on the fluorescence of the ROH* form, we conclude the following:

SCHEME 5

$$ROH^* \rightleftharpoons RO^{-*} + H^+$$

$$H^+ + B \xrightarrow{k'_{SC}} BH^+$$

1. A proton transferred from the excited chromophore to the hydrogen bonding network of the inner space of the protein may or may not permeate efficiently through the barrel and reach the solvent within the excited-state lifetime $\tau_f = 3.2$ ns. The time-resolved fluorescence results of GFP in the presence of a mild base in solution indicate that the proton scavenging process is not effective.

2. Relatively large size weak bases, like acetate or $H_2PO_4^-$, and even a smaller base like F^-, cannot reach the interior of the WT-GFP and react with a proton. This agrees with the prediction of Remington that the barrel structure prevents a good connection between the inner part of the protein with the solvent and also the large ions surrounding the protein. We note that in other studies of proton transfer in solution, Nachliel and Gutman[43] come to similar conclusions about the magnitude of proton diffusion in gramicidin. It thus appears that a random-walk model, despite the rather ornate and geometrically restricted active site of the GFP protein, provides an approximate description of the proton-transfer dynamics.

Acknowledgment. We acknowledge Professor S. J. Remington for his generous gift of WT-GFP. We thank Professor N. Agmon for his helpful and fruitful suggestions and discussions. We thank Professor M. Gutman for his helpful discussions. This work was supported by grants from the Binational US-Israel Science Foundation, the U. S. National Foundation and the James-Franck German-Israel Program in Laser-Matter Interaction.

References and Notes

(1) Weller, A. *Prog. React. Kinet.* **1961**, *1*, 189.
(2) (a) Solntsev, K. M.; Huppert, D.; Agmon, N.; Tolbert, L. M. *J. Phys. Chem. A*, **2000**, *104*, 4658. (c) Tolbert, L. M.; Solntsev, K. M. *Acc. Chem. Res.* **2002,** *35*, 19.
(3) Ireland, J. F.; Wyatt, P. A. H. *Adv. Phys. Org. Chem.* **1976**, *12*, 131.
(4) Förster, Th.; *Pure Appl. Chem.* **1970**, *24*, 443.
(5) Gutman, M.; Nachliel, E. *Biochim. Biophys. Acta*, **1990**, *391*, 1015.
(6) Schulman, S. G. In *Modern Fluorescence Spectroscopy*: Wehry, E. L., Ed.; Plenum: New York, 1975, Vol. 2, p 239.
(7) Huppert, D.; Gutman, M.; Kaufmann, K. J. In *Advances in Chemical Physics*; Jortner, J., Levine, R. D., Rice, S. A., Eds.; Wiley: New York, 1981; Vol. *47*, 681; Kosower, E.; Huppert, D. In *Annual Reviews of Physical Chemistry*; Strauss, H. L., Babcok, G. T., Moore, C. B., Eds.; Annual Reviews Inc: 1986; Vol. 37, 122.
(8) Pines, E.; Pines, D. In *Ultrafast Hydrogen Bonding Dynamics and Proton-Transfer Processes in the Condensed Phase*; Elsaesser, T., Bakker, H. J., Eds.; Kluwer Academic Publishers: Netherlands, 2002, 155−184.
(9) Agmon, N.; Pines E.; Huppert, D. *J. Chem. Phys.* **1988**, *88*, 5631.
(10) Pines, E.; Huppert, D.; Agmon, N. *J. Chem. Phys.* **1988**, *88*, 5620.
(11) Cubitt, A. B.; Heim, R.; Adams, S. R.; Boyd, A. E.; Gross, L. A.; Tsien, R. Y. *Trends Biochem. Sci.* **1995**, *20*, 448.
(12) Ormö, M.; Cubitt, A. B.; Kallio, K.; Gross, L. A.; Tsien, R. Y.; Remington, S. J. *Science* **1996**, *273*, 1392.
(13) Yang, F.; Moss, L. G.; Phillips, G. N. J. *Nat. Biotech.* **1996**, *14*, 1246.
(14) Brejc, K.; Sixma, T. K.; Kitts, P. A.; Kain, S. R.; Tsien, R. Y.; Ormö, M.; Remington, S. J. *Proc. Natl. Acad. Sci. U.S.A.* **1997**, *94*, 2306.
(15) Chattoraj, M.; King, B. A.; Bublitz, G. U.; Boxer, S. G. *Proc. Natl. Acad. Sci. U.S.A.* **1996**, *93*, 8362.
(16) (a) Lossau, H.; Kummer, A.; Heinecke, R.; Pollinger-Dammer, F.; Kompa, C.; Bieser, G.; Jonsson, T.; Silva, C. M.; Yang, M. M.; Youvan, D. C.; Michel-Beyerle, M. E. *Chem. Phys.* **1996**, *213*, 1. (b) Kummer, A.

D.; Kompa, C.; Lossau, H.; Pollinger-Dammer, F.; Michel-Beyerle, M. E.; Silva, C. M.; Bylina, E. J.; Coleman, W. J.; Yang, M. M.; Youvan, D. C. *Chem. Phys.* **1998**, *237*, 183.

(17) Striker, G.; Subramanian, V.; Seidel, C. A. M.; Volkmer, A. *J. Phys. Chem. B* **1999**, *103*, 8612.

(18) Winkler, K.; Lindner, J. R.; Subramanian, V.; Jovin, T. M.; Vohringer, P. *Phys. Chem. Chem. Phys.* **2002**, *4*, 1072.

(19) Litvinenko, K. L.; Webber, N. M.; Meech, S. R. *Bull. Chem. Soc. Jpn.* **2002**, *75*, 1065.

(20) Cotlet, M.; Hofkens, J.; Maus, M.; Gensch, T.; Van der Auweraer, M.; Michiels, J.; Dirix, G. Van Guyse, M.; Vanderleyden, J.; Visser, A. J. W. G.; De Schryver, F. C. *J. Phys. Chem. B* **2001**, *105*, 4999.

(21) Heikal, A. A.; Hess, S. T.; Webb, W. W. *Chem. Phys.* **2001**, 274, 37.

(22) Haupts, U.; Maiti, S.; Schwille, P.; Webb, W. W. *Proc. Natl. Acad. Sci. U.S.A.* **1998**, *95*, 13573.

(23) Debye, P. *Trans. Electrochem. Soc.* **1942**, *82*, 265

(24) Poles, E.; Cohen, B.; Huppert, D. *Israel J. Chem.* **1999**, *39*, 347.

(25) Krissinel, E. B.; Agmon, N. *J. Comput. Chem.* **1996**, *17*, 1085.

(26) Bransburg-Zabary, S.; Nachliel, E.; Gutman, M. *Biophys. J.* **2002**, 83, 2987.

(27) Kerr, I. D.; Sansom M. S. P. *Biophys. J.* **1996**, 70, 1643.

(28) Agmon, N.; Goldberg, S. Y.; Huppert, D. *J. Mol. Liq.* **1995**, *64*, 161.

(29) To follow the nonexponential tail, accurate data measurements are required. This might depend on the laser excitation system and TCSPC measuring system. We also measured the GFP fluorescence at both bands by a similar system of Prof. E. Haas at the life sciences department Bar-Ilan University. We found out that the time-resolved luminescence measurements of the samples were identical in both samples.

(30) Since samples can deteriorate and hence the measurements are invalid, we used another source of WT-GFP samples, from the lab of Prof. M. Gurevitz, Faculty of life sciences, Tel-Aviv University. We found out that the time-resolved fluorescence curves of both bands were almost identical, both GFP samples had the power law decay of $t^{-3/2}$ decay.

(31) Pines, E.; Pines, D.; Barak, T.; Magnes, B. Z.; Tolbert, L. M.; Haubrich, J. E. *Ber. Buns. Phys. Chem.* **1998**, *102*, 511.

(32) Scharnagl, C.; Raupp-Kossmann, R.; Fischer, S. F. *Biophys. J.* **1999**, *77*, 1839.

(33) Gopich, I. V.; Solntsev, K. M.; Agmon, N. *J. Chem. Phys.* **1999**, 110, 2164.

(34) Solntsev, K. M.; Huppert, D.; Agmon, N. *Phys. Rev. Lett.* **2001**, 86, 3427.

(35) Molotsky, T.; Huppert, D. *J. Phys. Chem. A* **2002**, *106*, 8525.

(36) Agmon, N. *J. Phys. Chem. A* **2002**, *106*, 7256.

(37) Eigen, M.; Kruse, W.; Maas, G.; De Maeyer, L. *Prog. React. Kinet.* **1964**, *2*, 287.

(38) Fraunfelder, H. *J. Phys. Chem.* **1990**, *94*, 1024.

(39) Agmon, N.; Hopfield, J. J. *J. Chem. Phys.* **1983**, *78*, 6947.

(40) Cohen, B.; Huppert, D.; Solntsev, K. M.; Nachliel E.; Tsfadia, Y.; Gutman, M. *J. Am. Chem. Soc.* **2002**, *124*, 7539.

(41) Goldberg, S. Y.; Pines, E.; Huppert, D. *Chem. Phys. Lett.* **1992**, *192*, 77.

(42) Huppert, D.; Cohen, B.; Agmon, N. *J. Am. Chem. Soc.* **2000**, *122*, 9838.

(43) Gutman, M.; Nachliel, E. *Annu. Rev. Phys. Chem.* **1997**, *48*, 329.